Analyzing powers and the role of multistep processes in the ^{12}C(^{7}Li, t)^{16}O reaction

W. D. Weintraub,[1,*] N. Keeley,[2,†] K. W. Kemper,[1,3] K. Kravvaris,[1,‡] F. Maréchal,[4] D. Robson,[1]
B. T. Roeder,[1,§] K. Rusek,[3] and A. Volya[1]

[1]*Department of Physics, Florida State University, Tallahassee, Florida 32306, USA*
[2]*National Centre for Nuclear Research, ul. Andrzeja Sołtana 7, 05-400 Otwock, Poland*
[3]*Heavy Ion Laboratory, University of Warsaw, ul. Pasteura 5a, 02-093 Warsaw, Poland*
[4]*Institut de Physique Nucléaire, CNRS-IN2P3, Université Paris-Sud, Université Paris-Saclay, 91406 Orsay, France*

The analyzing powers ${}^T T_{10}$, ${}^T T_{20}$, and ${}^T T_{30}$ for the ^{12}C(^{7}Li, t) reaction were measured and combined with new and previously determined angular distributions to probe the role of multistep processes through coupled channel Born approximation (CCBA) calculations employing new α-particle spectroscopic amplitudes calculated with the phenomenological shell model in the unrestricted *psd* space. Good descriptions of the cross-section angular distributions could be obtained except for the larger angles for the 6.05 MeV 0^+ and 6.13 MeV 3^- states, while the analyzing powers were not generally described. The calculations presented demonstrate the sensitivity of the angular distributions of both the differential cross sections and the analyzing powers to various multistep routes. While the measured analyzing power ${}^T T_{30}$ is roughly zero for all states, the various CCBA calculations produced large and highly oscillatory values for this observable, showing that other multistep processes must be present beyond those taken into account in this work. Standard distorted wave Born approximation (DWBA) calculations were also carried out and these show considerable differences from the CCBA results but the description of the analyzing powers, while slightly improved, is still poor.

I. INTRODUCTION

The utility of Li beams for studying nuclear properties was recognized early on in nuclear reaction studies with accelerators. The possibility of using the ^{7}Li(^{7}Li, p) reaction to produce ^{13}B was demonstrated when an ion source capable of producing ^{7}Li beams was developed for the University of Chicago 2-MeV Van de Graaff [1]. Subsequently, this machine was used to probe the ^{7}Li(^{6}Li, d)^{11}B and ^{6}Li(^{7}Li, t)^{10}B reactions where it was shown that the angular distributions were forward peaked [2]. By interchanging the target and beam to measure the large angles via the ^{6}Li(^{7}Li, d)^{11}B and ^{7}Li(^{6}Li, t)^{10}B processes, it was demonstrated that both the (^{6}Li, d) and (^{7}Li, t) reactions were asymmetric about $90°$, which was interpreted as showing that an α particle was transferred from the Li projectile to the target. The $\alpha + t$ cluster structure of ^{7}Li was clearly shown experimentally through the ^{3}H(α, γ) capture reaction [3]. The $\alpha + {}^3$He cluster structure of ^{7}Be was also demonstrated in the same work. Theoretical work on the cluster structure of the Li nuclei built upon that of Wheeler [4] and later Wildermuth and coworkers [5]. At roughly the same time, the interaction of ^{6}Li beams of energies 30 and 60 MeV with ^{197}Au targets was being investigated,

and it was found that copious amounts of α particles were produced and they were attributed to Coulomb dissociation of the beam [6]. However, the early success of the possible direct transfer shown in Ref. [2] suggested that it might be possible to determine the α-particle reduced width for the 7.12 MeV 1^- state in ^{16}O by the ^{12}C(^{6}Li, d) reaction at higher bombarding energies. Unfortunately, no deuterons corresponding to the ^{16}O ground state were detected at the two energies studied, 36 and 63 MeV [7], and it was proposed that the observed continuum of deuterons arose from the breakup of ^{6}Li. Part of the problem with the high energy studies was the poor beam energy resolution of 600 keV. The development of heavy-ion sources for tandem Van de Graaff accelerators with their higher beam energies compared with the early single ended machines, when coupled with magnetic spectrographs allowed the exploration of α structures in the light nuclei ^{16}O and ^{20}Ne. The published spectra [8] clearly demonstrated the selectivity of the ^{12}C, ^{16}O(^{6}Li, d) and (^{7}Li, t) reactions with only very weak population of the unnatural parity 2^- state at 8.87 MeV in ^{16}O. However, it was the stronger population of this state by (^{6}Li, d) when compared with that by (^{7}Li, t) and the lack of population of the 4.97 MeV 2^- in ^{20}Ne [8,9] that led to the speculation that the (^{7}Li, t) reaction would be the best α-transfer reaction for probing the α widths of states in ^{16}O. An excellent early review of both Li ion sources and reaction studies of Li induced α-transfer reactions was given by Bethge [10].

The fact that the α particle and triton are in a relative $L = 1$ state in ^{7}Li means that the (^{7}Li, t) reaction could not be handled by the zero-range distorted wave Born approximation

_____
*Deceased.

†Corresponding author: nicholas.keeley@ncbj.gov.pl

‡Permanent address: Lawrence Livermore National Laboratory, Livermore, CA 94551, USA.

§Permanent address: Cyclotron Institute, Texas A&M University, College Station, TX 77843, USA.

(DWBA) treatment available at the time of the early studies, which led to extensive measurements of the ^{12}C(^{6}Li, d) reaction at several energies. In addition, considerable effort was put into determining the possible compound nucleus (CN) contributions to the observed cross sections [11,12]. While the weak population of the unnatural parity 2$^-$ state at 8.87 MeV led to the claim of a CN contribution to the (^{6}Li, d) reaction this possibility was reinforced by the strong population of the 3$^+$, 4$^+$ doublet at 11.09 MeV. The unnatural parity 11.080 MeV 3$^+$ state cannot be populated by a direct α transfer and the 11.097 4$^+$ state has a small α-decay width and so again would not be expected to be significantly populated by direct α transfer. However, Ref. [8] showed that it is the 11.097 MeV state that is populated and this work was later reinforced by high resolution data [13] and a direct measurement by particle-γ means to obtain the 3$^+$ cross section [14]. The conclusion of these works was that it is the 11.097 MeV 4$^+$ state which is predominantly populated in the ^{12}C(^{6}Li, d) reaction, with the 3$^+$ cross section at least a factor of 5 weaker, so compound nucleus calculations that were matched to the combined levels at 11.09 MeV over predicted the CN contribution to the (^{6}Li, d) reaction.

Another explanation for the population of unnatural parity states is that they are produced via multistep processes through the excitation of states in ^{6}Li and/or ^{12}C followed by transfer, as suggested in Refs. [13,15]. To study this possibility, analyzing powers for the ^{12}C(^{6}Li, d) reaction were measured for both rank 1 and 2 polarized ^{6}Li beams at energies of 34 and 50 MeV [16]. This work showed that the population of the 6.92 MeV 2$^+$ and 10.35 MeV 4$^+$ states was via direct α transfer but that significant multistep contributions were present in the transfers to the 0$^+$ ground and 6.13 MeV 3$^-$ states. The main issue raised in this work was the sensitivity of the calculations to the signs of the multistep transfer amplitudes which are poorly known.

The increased selectivity of the ^{12}C(^{7}Li, t) reaction and the possibility that this might be a "true" α transfer spurred a series of measurements at energies of 15, 21.1 and 24 MeV with the lower two energies allowing clean separation between the 6.92 MeV 2$^+$ and 7.12 MeV 1$^-$ levels [17]. The data showed strong forward peaking for all observed angular distributions, including that to the 8.87 MeV 2$^-$, with angles greater than 90° being described by Hauser-Feshbach compound nucleus calculations that assumed triton emission from the intermediate ^{19}F. While true finite range calculations were not possible at the time, they were approximated and described the angular distributions quite well. While the population of the 2$^-$ 8.87 MeV level was weak the question was whether carrying out a reaction study at higher beam energies would result in a more direct α transfer reaction, which resulted in a detailed study at 38 MeV [18]. An interesting observation is immediately apparent when the cross sections for producing the 6.92 MeV 2$^+$ state at 24 and 38 MeV are compared. That at the lower energy is a factor of four larger than at the higher energy. This difference reflects the fact that the reaction is less well angular momentum matched at the higher energy and at 38 MeV this favors the population of the 10.35 MeV 4$^+$ state. In addition, the (^{6}Li, d) reaction is more poorly angular momentum matched in general than the

(^{7}Li,t) reaction which again favors the latter for extracting α spectroscopic factors.

The focus of a detailed study of the ^{12}C(^{7}Li, t) reaction, carried out at 34 MeV with the energy resolution necessary to separate the 6.92 MeV 2$^+$ and 7.12 MeV 1$^-$ states, was to extract spectroscopic factors and reduced widths for these and other states in ^{16}O [19] through finite-range distorted-wave Born approximation (FRDWBA) calculations. The sensitivity to the various parameters needed to carry out these FRDWBA calculations then led more recently to a sub-Coulomb (^{6}Li, d) and (^{7}Li, t) study to extract the reduced widths for these same 2$^+$ and 1$^-$ states [20]. New measurements and analysis of the (^{7}Li, t) reaction at 28 and 34 MeV were carried out due to the wide range of values obtained for the extracted α spectroscopic factors and hence reduced widths for the population of states in ^{16}O [21]. The use of a magnetic spectrograph as in Ref. [19] again resulted in clean separation of the two states of most interest. Measurement of two energies allows for a check on the HF and FRDWBA calculations used to extract the spectroscopic factors.

One of the concerns raised in previously published work is the possibility of multistep contributions to the calculated cross sections as evidenced by the population of the 8.87 MeV 2$^-$ level, which could affect the extracted α-spectroscopic factors. Early coupled channel Born approximation (CCBA) calculations by Cobern *et al.* [18] resulted in little effect on the extracted spectroscopic factors for the 6.92 MeV 2$^+$ and 10.35 MeV 4$^+$ states but they were not performed for other states populated in ^{16}O. The present work reports first, second and third rank analyzing powers measured with a polarized ^{7}Li beam at a beam energy of 34 MeV. New absolute cross sections were also obtained and are combined with those of Refs. [19] and [21]. CCBA calculations with spectroscopic amplitudes from a modern shell model calculation are then used to investigate the role of both direct and multistep contributions to the ^{12}C(^{7}Li, t) reaction.

II. EXPERIMENTAL METHOD

Data were taken with both unpolarized and polarized 34 MeV ^{7}Li beams supplied by the FSU tandem accelerator of the J. D. Fox Laboratory. The beam for the unpolarized runs, carried out to determine the absolute cross sections for the ^{12}C(^{7}Li, t) reaction, was produced by a sputter source. The experimental set up comprised a 100 μg/cm^2 natural carbon target and two ΔE-E telescopes consisting of 500 μm ΔE and 5-mm-thick E Si detectors subtending an opening angle of 0.25°. A monitor detector was used to check the accuracy of the beam integration. The thickness of the ΔE detectors was such that the elastically scattered ^{7}Li were stopped so that it was possible to extract absolute cross sections for both the scattering and reaction data by normalizing to previously determined elastic scattering cross sections [22]. The total error in the absolute elastic scattering cross section in Ref. [22] was ±7% and since the major error here arises from the detector absolute angle calibration, done in the same way as Ref. [22], the absolute error for the elastic scattering is ±10% when the possible angle setting error is included. Combining this error with that for counting statistics increases the overall
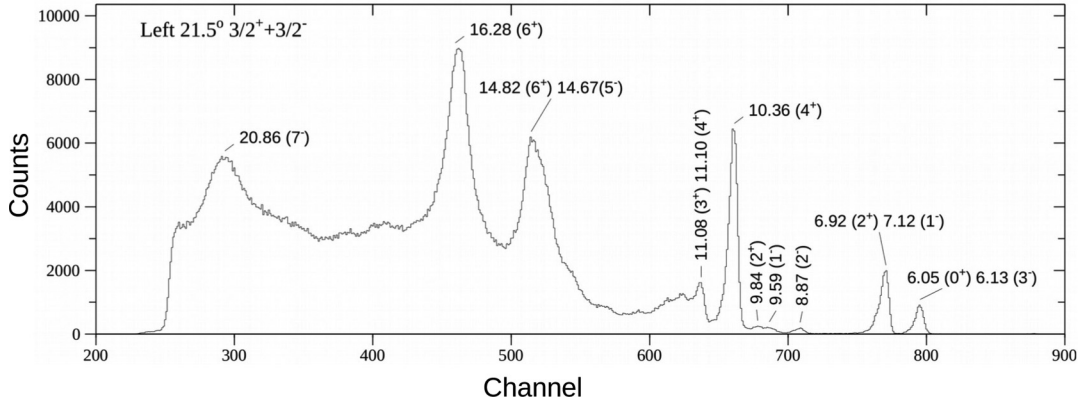
FIG. 1. Typical spectrum of outgoing tritons recorded during the polarized beams runs indicating the states in ^{16}O observed. The spectrum is the sum of the results for two different beam polarization states (effectively amounting to an unpolarized spectrum) for the detector on the left-hand side of the beam axis at a scattering angle of $\theta_{\text{lab}} = 21.5°$. The ^{16}O ground-state peak has been omitted for the sake of clarity.

uncertainty in the absolute cross section to $\pm 12\%$ for the $(^7\text{Li}, t)$ reaction.

The polarized ^{7}Li beam was produced by the FSU optically pumped ion source. A description of the system and the beam polarizations has been given by Cathers *et al.* [23,24] and Bartosz *et al.* [25]. The beam polarizations on target were $t_{10} = 0.50 \pm 0.02$, $t_{20} = 0.49 \pm 0.02$ and $t_{30} = 0.46 \pm 0.03$. The beam polarizations were monitored throughout by use of the $\alpha(^7\text{Li}, \alpha)^7\text{Li}^*_{4.63 \text{ MeV}}$ reaction which was previously shown to have large analyzing powers [23]. The differences between the present work and that of Bartosz *et al.* [25], who measured the analyzing powers for ^{7}Li scattering by ^{12}C, were that the detector opening angle was increased to $1.1°$ and the four ΔE-E telescopes consisted of 500 μm ΔE detectors with 5-mm E detectors, as in the unpolarized cross section runs. The target thickness was 400 μg/cm^2. While the thicker target degraded the energy resolution of the final triton spectrum it was necessary to be able to acquire sufficient statistics for a meaningful determination of the reaction analyzing powers. One consequence of the degraded energy resolution was that in the polarized beam runs the 6.05 MeV 0^+_2 and 6.13 MeV 3^-_1 and the 6.92 MeV 2^+_1 and 7.12 MeV 1^-_1 states of ^{16}O could not be separated and analyzing powers for the two doublets were recorded. However, the 6.13 MeV 3^-_1 and 6.92 MeV 2^+_1 contributions are expected to dominate due to their larger cross sections. Figure 1 shows a typical spectrum of the outgoing tritons recorded during the polarized beam runs.

The cross section angular distributions presented in Sec. IV B are the combined results of the present measurements and those of Refs. [19] and [21]. The absolute values of the cross sections of Ref. [19] were consistently somewhat smaller than those of Ref. [21] and the present work, which agreed with each other, hence they were normalized to the values of Ref. [21]. For points where the scattering angles were identical to within $1.0°$ for the different data sets the error-weighted mean was taken. Since the statistics of the present measurements using the thin target were relatively poor only the cross section results for the 0.0 MeV 0^+_1, 8.87 MeV 2^-_1, and 10.35 MeV 4^+_1 states obtained with the thick target were combined with the existing measurements.

III. SHELL MODEL CALCULATIONS

The nuclear many-body wave functions for ^{16}O and ^{12}C are obtained from the phenomenological shell model in the unrestricted *psd* space, where all possible multiparticle-multihole excitations are included. We use the interaction described in [27], which was designed specifically to describe the non-closed-core components of the ^{16}O wave function, and has been found to provide an accurate description of both the spectra and the reduced α widths for the $^{16}\text{O} \rightarrow {}^{12}\text{C}(\text{g.s.}) + \alpha$ system [26]. To facilitate the calculation of spectroscopic amplitudes, we define a reaction basis channel having the α particle and a state of ^{12}C in some relative harmonic oscillator (HO) motion $\phi_{n\ell}$, with a maximum number of quanta constrained by the *psd* space choice. Thus, each basis channel is defined by the quantum numbers $\{\beta n \ell J\}$, where β denotes the ^{12}C state (here either the ground state or the first 2^+ state), n, ℓ are the number of nodes and angular momentum in the relative motion, and J is the total spin of the channel, obtained by coupling ℓ with the angular momentum of the ^{12}C state. The reaction basis channels are constructed using the method outlined in [28,29], exciting the center-of-mass (CM) HO motion of the α particle, which we treat as a closed s^4 core, and recoupling it with the desired ^{12}C state.

Due to the space selection, basis channels states have anywhere from 4 to 8 HO quanta in the relative motion, resulting in multiple nonorthogonal basis channels for each asymptotic quantum number set. The overlap norm kernel between the different basis channels contains all the information needed to obtain orthogonal reaction channels and is defined as

$$\mathcal{N}^{\beta \ell J}_{nn'} = \langle \Phi^J_{\beta n \ell} | \Phi^J_{\beta n' \ell} \rangle. \tag{1}$$

For each asymptotic quantum number set the norm kernel is diagonalized independently, and the phases of the resulting eigenvectors are fixed so that the maximal overlap with the basis channels is positive. This convention avoids any ambiguity arising from the freedom of choice in phase of the eigenvectors of the norm kernel matrix, a necessary step to obtain consistent phases between the various shell model states, and was chosen to reflect the fact that in the limit of

TABLE I. Spectroscopic amplitudes S_α, number of nodes n (including that at $r = 0$ but excluding that at $r = \infty$) and relative angular momentum ℓ for the various components of the $^{16}\text{O} = \alpha + {}^{12}\text{C}$ radial wave functions obtained from the shell model calculations.

^{16}O level	$^{12}\text{C}(0^+)$	$^{12}\text{C}(2^+)$
0_1^+	$n = 3,\ \ell = 0:\ S_\alpha = 0.76823$	$n = 2,\ \ell = 2:\ S_\alpha = 0.706533$
	$n = 4,\ \ell = 0:\ S_\alpha = -0.13807$	$n = 3,\ \ell = 2:\ S_\alpha = -0.538962$
	$n = 5,\ \ell = 0:\ S_\alpha = 0.430077$	$n = 4,\ \ell = 2:\ S_\alpha = 0.00317567$
0_2^+	$n = 3,\ \ell = 0:\ S_\alpha = 0.234481$	$n = 2,\ \ell = 2:\ S_\alpha = 0.210049$
	$n = 4,\ \ell = 0:\ S_\alpha = -0.430825$	$n = 3,\ \ell = 2:\ S_\alpha = -0.0659812$
	$n = 5,\ \ell = 0:\ S_\alpha = -0.542738$	$n = 4,\ \ell = 2:\ S_\alpha = 0.316571$
3_1^-	$n = 2,\ \ell = 3:\ S_\alpha = -0.78255$	$n = 3,\ \ell = 1:\ S_\alpha = -0.71144$
	$n = 3,\ \ell = 3:\ S_\alpha = 0.225505$	$n = 4,\ \ell = 1:\ S_\alpha = 0.228465$
		$n = 2,\ \ell = 3:\ S_\alpha = -0.749353$
		$n = 3,\ \ell = 3:\ S_\alpha = 0.238035$
		$n = 1,\ \ell = 5:\ S_\alpha = -0.667783$
		$n = 2,\ \ell = 5:\ S_\alpha = 0.0166371$
2_1^+	$n = 2,\ \ell = 2:\ S_\alpha = -0.00439515$	$n = 3,\ \ell = 0:\ S_\alpha = -0.396123$
	$n = 3,\ \ell = 2:\ S_\alpha = 0.184042$	$n = 4,\ \ell = 0:\ S_\alpha = -0.116413$
	$n = 4,\ \ell = 2:\ S_\alpha = 0.683085$	$n = 5,\ \ell = 0:\ S_\alpha = -0.200012$
		$n = 2,\ \ell = 2:\ S_\alpha = -0.02712$
		$n = 3,\ \ell = 2:\ S_\alpha = -0.164403$
		$n = 4,\ \ell = 2:\ S_\alpha = -0.0545063$
		$n = 1,\ \ell = 4:\ S_\alpha = -0.0170289$
		$n = 2,\ \ell = 4:\ S_\alpha = -0.217998$
		$n = 3,\ \ell = 4:\ S_\alpha = -0.140358$
1_1^-	$n = 3,\ \ell = 1:\ S_\alpha = 0.342384$	$n = 3,\ \ell = 1:\ S_\alpha = 0.524543$
	$n = 4,\ \ell = 1:\ S_\alpha = -0.182323$	$n = 4,\ \ell = 1:\ S_\alpha = -0.42106$
		$n = 2,\ \ell = 3:\ S_\alpha = 0.071797$
		$n = 3,\ \ell = 3:\ S_\alpha = 0.0905867$
4_1^+	$n = 1,\ \ell = 4:\ S_\alpha = 0.226227$	$n = 2,\ \ell = 2:\ S_\alpha = 0.357632$
	$n = 2,\ \ell = 4:\ S_\alpha = -0.404178$	$n = 3,\ \ell = 2:\ S_\alpha = -0.19278$
	$n = 3,\ \ell = 4:\ S_\alpha = 0.374127$	$n = 4,\ \ell = 2:\ S_\alpha = 0.002516$
		$n = 1,\ \ell = 4:\ S_\alpha = 0.037523$
		$n = 2,\ \ell = 4:\ S_\alpha = -0.125929$
		$n = 3,\ \ell = 4:\ S_\alpha = -0.167955$
		$n = 1,\ \ell = 6:\ S_\alpha = -0.322888$
		$n = 2,\ \ell = 6:\ S_\alpha = -0.039338$

$\mathcal{N}_{nn'}^{\beta\ell J} = \delta_{nn'}$, the basis channels already have a pre-determined phase with the wave function of the relative motion being positive as $\rho \to 0$. The maximal overlap is also used to determine the number of nodes in the relative wave function as the off-diagonal matrix elements of the norm kernel are relatively small, resulting in the expression

$$\left| \hat{\mathbf{\Phi}}_{\beta n \ell}^{J} \right\rangle = \sum_{n'} \mathcal{N}_{nn'}^{-1/2} \left| \Phi_{\beta n' \ell}^{J} \right\rangle \tag{2}$$

for the orthonormalized channels. Further to constrain the possible phase choices for the full channel, the phases of the ^{12}C shell-model wave functions are chosen such that the matrix element of the $E2$ transition operator is positive.

Finally, for each of the orthogonalized channels one can obtain the spectroscopic amplitude as the overlap with the corresponding ^{16}O parent state

$$S_\alpha = \left\langle \Psi(^{16}\text{O}) \middle| \hat{\mathbf{\Phi}}_{\beta n \ell}^{J} \right\rangle. \tag{3}$$

More details concerning the derivation of the orthonormalized basis and the construction of α particle relative basis channels can be found in [26,28]. The resulting spectroscopic amplitudes are given in Table I.

IV. REACTION CALCULATIONS

In this section we describe the calculation of the angular distributions for both cross sections and analyzing powers of the $^{12}\text{C}(^7\text{Li}, t)$ reaction populating the various levels in ^{16}O. We begin with a short discussion of the possible compound nucleus contributions and a description of the Hauser-Feshbach calculations performed to estimate them. The following two sections present the CCBA and FRDWBA calculations performed using the shell model $\langle ^{16}\text{O} \mid {}^{12}\text{C} + \alpha \rangle$ spectroscopic amplitudes. We present the CCBA calculations first for two, related, reasons: firstly, the CCBA formalism enables the inclusion of multistep transfer paths via excited states of the target and/or projectile and is therefore the more

complete calculation; secondly, in view of this fact the bound state potential well radius parameters for each state were adjusted to give the best description of the data by the CCBA calculations (this procedure is fully described in Sec. IV B).

A. Compound nucleus contributions

The use of the $^{12}C(^{6}Li, d)$ and $^{12}C(^{7}Li, t)$ reactions to probe the α-particle structure of ^{16}O has been plagued from the earliest days by the experimental population of the unnatural parity 2^- state at 8.87 MeV over a wide range of Li beam energies [8]. Population of this state via $(^{6}Li, d)$ was shown to have an angular distribution symmetric about $\theta_{c.m.} = 90°$, suggesting a compound nucleus mechanism. While this early work comparing the two reactions showed the population of the 2^- state to be relatively weaker in $(^{7}Li, t)$ than $(^{6}Li, d)$, it was still argued that possible compound nucleus contributions to the measured cross sections for individual states in ^{16}O could affect the extraction of spectroscopic information on α-particle clustering in ^{16}O and therefore needed to be taken into account. Klapdor *et al.* [30] presented the Hauser-Feshbach formalism and then applied it to light heavy-ion systems where it was shown that the overall magnitudes of the cross sections were sensitive to many of the parameters inherent in the calculations. However, determination of the critical angular momentum of the fusing system then makes it possible to establish parameters of the compound system such as level densities and even final state spins. Dennis *et al.* [31] showed

TABLE II. Woods-Saxon potential well radii used to calculate the various components of the $^{16}O = \alpha + {}^{12}C$ radial wave functions employed in the CCBA and DWBA calculations.

^{16}O level	Radius R (fm)
0.00 MeV 0_1^+	2.50
6.05 MeV 0_2^+	4.70
6.13 MeV 3_1^-	2.10
6.92 MeV 2_1^+	3.30
7.12 MeV 1_1^-	3.20
10.35 MeV 4_1^+	3.30

that by using fusion cross sections for the $^{12}C + {}^{7}Li$ system it was possible to determine the critical angular momentum ℓ_{cr} of the fusing system and hence the total critical angular momentum of the system J_{cr} to within one unit of $\hbar$. With this information it then becomes possible to predict absolute Hauser-Feshbach (HF) compound nucleus cross sections to within $\pm 30\%$. To test this idea Dennis *et al.* measured angular distributions for the $^{12}C(^{7}Li, t)$ reaction using direct kinematics at forward angles and inverse kinematics at large angles to provide data over the whole angular range to be compared with the computed cross sections that used the value of ℓ_{cr} extracted from the fusion data. The fact that the calculations described the absolute magnitude of the data then validated this procedure. A further test was to compare the computed
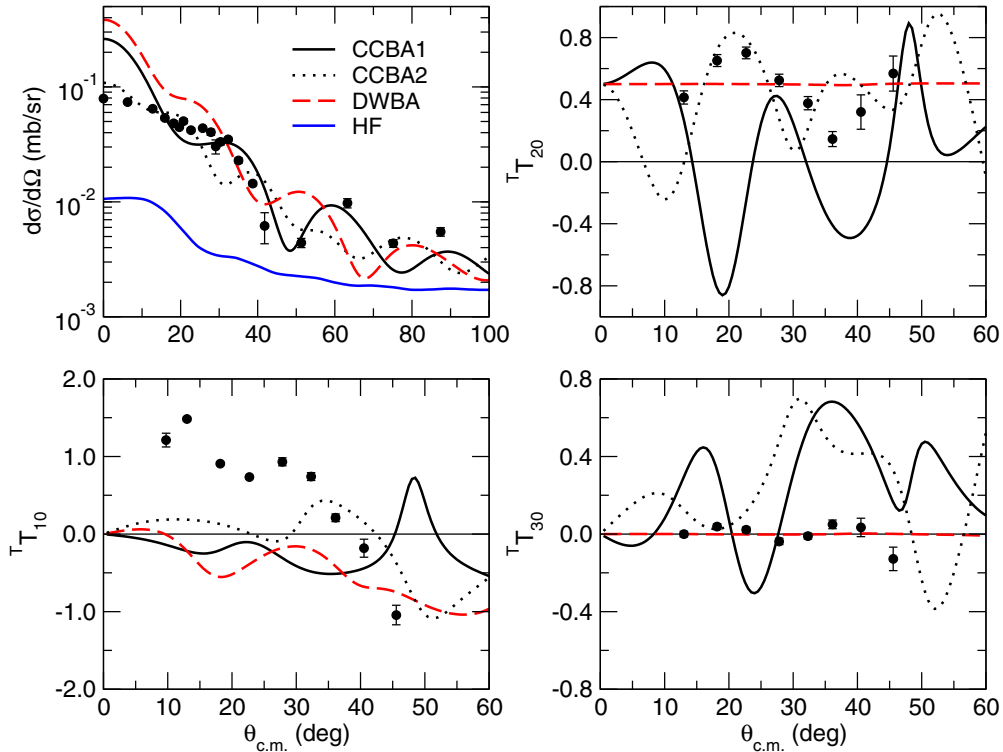

FIG. 2. Cross section and analyzing power angular distributions for the $^{12}C(^{7}Li, t)^{16}O$ reaction to the 0.0 MeV 0_1^+ state of ^{16}O. The solid black curves denote the CCBA calculation including ground state reorientation and excitation of the 0.478 MeV $1/2^-$ state of ^{7}Li and excitation of the 4.44 MeV 2^+ state of ^{12}C (CCBA1), the dotted black curves the CCBA calculation with additional coupling to the 4.63 MeV $7/2^-$ resonance of ^{7}Li (CCBA2) and the dashed red curve the DWBA calculation. The solid blue curve denotes the Hauser-Feshbach compound nucleus cross section calculated with HELGA which was added incoherently to the CCBA and DWBA cross sections.
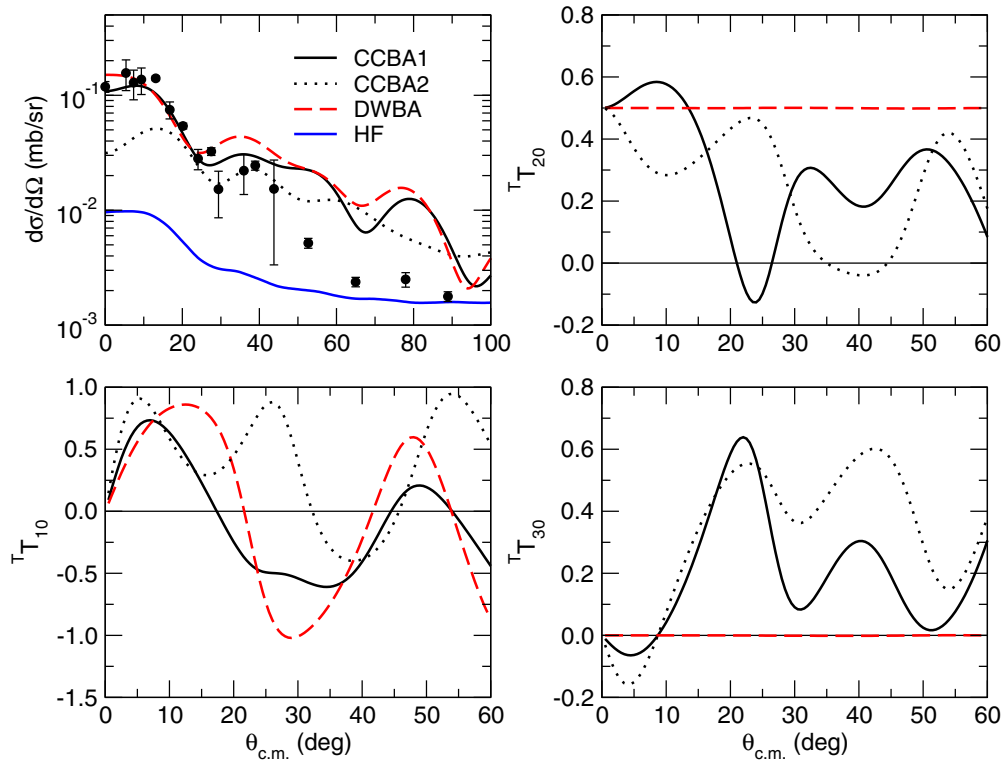
FIG. 3. Cross section and analyzing power angular distributions for the ^{12}C(^{7}Li, t)^{16}O reaction to the 6.05 MeV 0_2^+ state of ^{16}O. The solid black curves denote the CCBA calculation including ground state reorientation and excitation of the 0.478 MeV $1/2^-$ state of ^{7}Li and excitation of the 4.44 MeV 2^+ state of ^{12}C (CCBA1), the dotted black curves the CCBA calculation with additional coupling to the 4.63 MeV $7/2^-$ resonance of ^{7}Li (CCBA2) and the dashed red curve the DWBA calculation. The solid blue curve denotes the Hauser-Feshbach compound nucleus cross section calculated with HELGA which was added incoherently to the CCBA and DWBA cross sections.

HF cross sections with the previously published ^{12}C(^{7}Li, t) data of Pühlofer *et al.* [17] at 24 MeV and that of Cobern *et al.* [18] at 38 MeV. The comparisons showed that at a bombarding energy of 24 MeV all states, including the 8.87 MeV 2^-, had forward angle cross sections significantly larger than those arising from the compound nucleus process whereas at 38 MeV the 8.87 MeV cross section was completely described by the HF calculation.

The parameters given in Ref. [31] were used in the legacy compound nucleus code HELGA [32] to determine the CN contributions to the 34 MeV ^{12}C(^{7}Li, t) data presented here. The extracted ℓ_{cr} as given in Table 1 of Ref. [31] is $10 \pm 1\hbar$, which then determines J_{cr} to be in the range 10, 11 or 12$\hbar$. The magnitude of the 8.87 MeV 2^- cross section is reproduced with $J_{cr} = 10\hbar$ and this value was used to determine the compound nucleus contributions to the data presented in this work. The only transfer for which the compound contribution will impact the extraction of spectroscopic information is that to the ground state, where it is at most 10%.

B. Coupled channel Born approximation calculations

The CCBA calculations were performed with the code FRESCO [33]. Couplings to the 4.44 MeV 2^+ excited state of ^{12}C and the 0.478 MeV $1/2^-$ state of ^{7}Li, plus reorientation of the $3/2^-$ ground state were included in the main set of calculations. The ^{12}C states were treated as members of an oblate

$K = 0$ rotational band, with the Coulomb coupling strength taken from Ref. [34] and the nuclear deformation length, $\delta_2 = -1.20$ fm, obtained by adjusting to fit the inelastic scattering data of Ref. [35]. The ^{7}Li states were treated as members of a prolate $K = 1/2$ band, with the Coulomb coupling strength taken from Ref. [36] and the nuclear deformation length, $\delta_2 = 2.0$ fm, obtained by adjusting to fit the inelastic scattering data of Ref. [35]. The entrance channel optical potential parameters were obtained using set VII of Table I of Ref. [22] as a starting point and adjusting to fit the elastic scattering data of Ref. [22] in a coupled channel calculation including the projectile and target inelastic excitations. The resulting values were: $V = 277.9$ MeV, $r_V = 0.638$ fm, $a_V = 0.740$ fm, $W = 9.16$ MeV, $r_W = 1.239$ fm, and $a_W = 0.924$ fm, both real and imaginary potentials being of volume Woods-Saxon form with the radius convention $R_x = r_x(A_p^{1/3} + A_t^{1/3})$. The Coulomb radius parameter was held fixed at $r_C = 1.25$ fm. The exit channel $t + {}^{16}$O optical potentials employed the HT1p global parameters of Ref. [37], specifically adapted to 1p-shell targets.

The transfer steps were performed within the post form of the DWBA formalism and included the full complex remnant term. The $\alpha + t$ binding potentials were taken from Ref. [38]. The spectroscopic amplitudes for the $\langle {}^7\text{Li}(3/2^-) | \alpha + t \rangle$ and $\langle {}^7\text{Li}(1/2^-) | \alpha + t \rangle$ overlaps were set to $+1.0$ and -1.0, respectively. The negative sign for the $\langle {}^7\text{Li}(1/2^-) | \alpha + t \rangle$ spectroscopic amplitude was found to be crucial to
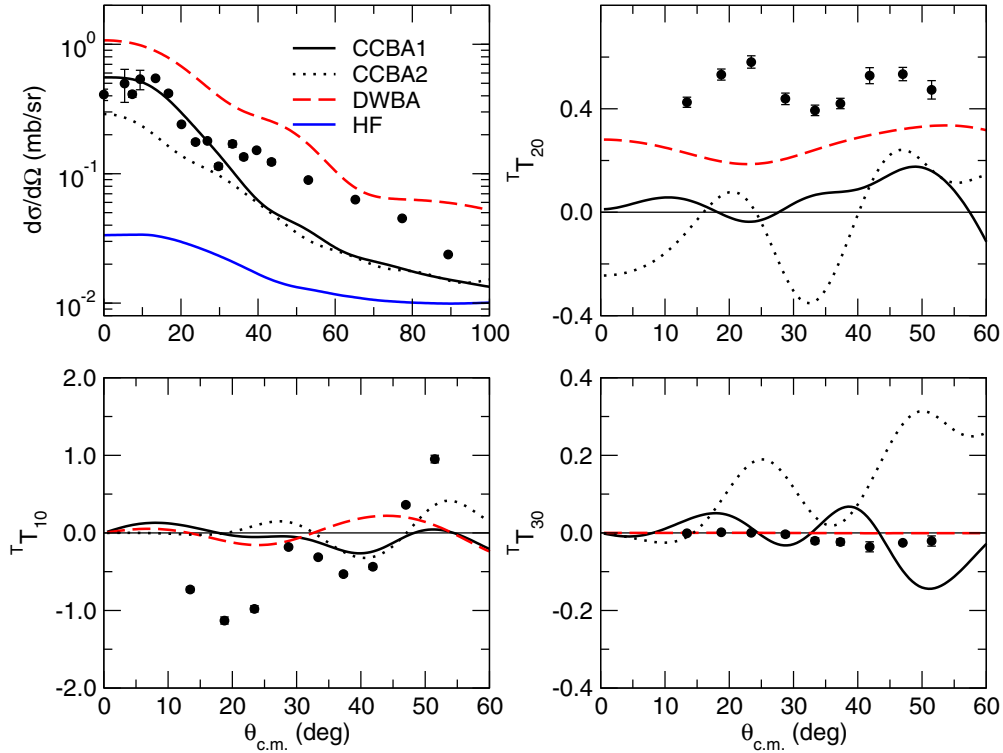
FIG. 4. Cross section and analyzing power angular distributions for the ^{12}C(^{7}Li, t)^{16}O reaction to the 6.13 MeV 3_1^- state of ^{16}O. The solid black curves denote the CCBA calculation including ground state reorientation and excitation of the 0.478 MeV $1/2^-$ state of ^{7}Li and excitation of the 4.44 MeV 2^+ state of ^{12}C (CCBA1), the dotted black curves the CCBA calculation with additional coupling to the 4.63 MeV $7/2^-$ resonance of ^{7}Li (CCBA2) and the dashed red curve the DWBA calculation. The solid blue curve denotes the Hauser-Feshbach compound nucleus cross section calculated with HELGA which was added incoherently to the CCBA and DWBA cross sections. The calculated analyzing powers are the cross section weighted means of the analyzing powers for the 6.05 MeV 0_2^+ and 6.13 MeV 3_1^- states, see text for details.

reproducing the transfer data and is in agreement with the calculations of Ref. [39]. The spectroscopic amplitudes for the $\langle ^{16}$O $\mid \alpha + {}^{12}$C$(0^+) \rangle$ and $\langle ^{16}$O $\mid \alpha + {}^{12}$C$(2^+) \rangle$ overlaps were taken from the shell model calculation results given in Table I. The transferred α particle was bound to the ^{12}C core in a Woods-Saxon well of diffuseness $a = 0.55$ fm and radius adjusted to give the best description of the transfer data to each individual ^{16}O state. The resulting values are given in Table II. The rather large variation in R between the 0_1^+ and 0_2^+ states probably reflects the different structure of these two levels. The significantly larger radius required for the 6.05 MeV 0_2^+ state compared to the 0_1^+ ground state is consistent with the wave functions of both conventional ^{12}C $+ \alpha$ and five-body ^{12}C $+ ppnn$ orthogonality condition model (OCM) calculations presented in Ref. [40]; the relevant components of the present wave functions are actually in quite good quantitative agreement with the conventional OCM radial wave functions presented in Figs. 1 and 3 of Ref. [40]. The well depths were adjusted to give the appropriate binding energy for each state, with the exception of the 10.35 MeV 4^+ level where the α particle is unbound with respect to the ^{12}C core in its 0^+ ground state; in this case the weak binding energy approximation was used and the wave function was calculated assuming a binding energy of 0.001 MeV (the correct excitation energy was, however, used in the "kinematic" part of the calculation).

The results of these calculations, the solid black curves labeled "CCBA1," are compared with the data in Figs. 2– 8. Also shown are the compound nucleus contributions to the cross sections calculated with the code HELGA, which were added incoherently to the CCBA cross sections. The description of the cross section angular distributions is good, with the exception of the 6.05 MeV 0_1^+ and 6.13 MeV 3_1^- states for angles $\theta_{c.m.} > 30°$. However, the analyzing powers are in general not well described. Recall that the measured analyzing powers plotted in Figs. 4 and 5 actually represent the results for the unresolved doublets of the 6.05 MeV 0_2^+ and 6.13 MeV 3_1^- and 6.92 MeV 2_1^+ and 7.12 MeV 1_1^- states, respectively. The solid black curves on these figures therefore denote the cross section weighted means of the calculated analyzing powers for both members of the doublet.

A further set of CCBA calculations was performed where excitation of the 4.63 MeV $7/2^-$ resonance of ^{7}Li, together with α-particle transfer from this state, was added. The excitation of this level was calculated assuming that it was the next member of the $K = 1/2$ band. The spectroscopic amplitude for the $\langle ^7$Li$(7/2^-) \mid \alpha + t \rangle$ overlap was set to -1.0, the sign again being in agreement with the calculations of Ref. [39]. Since the α particle is unbound with respect to the ^{3}H "core" in this state the weak binding energy approximation was employed to calculate the bound state radial wave function with
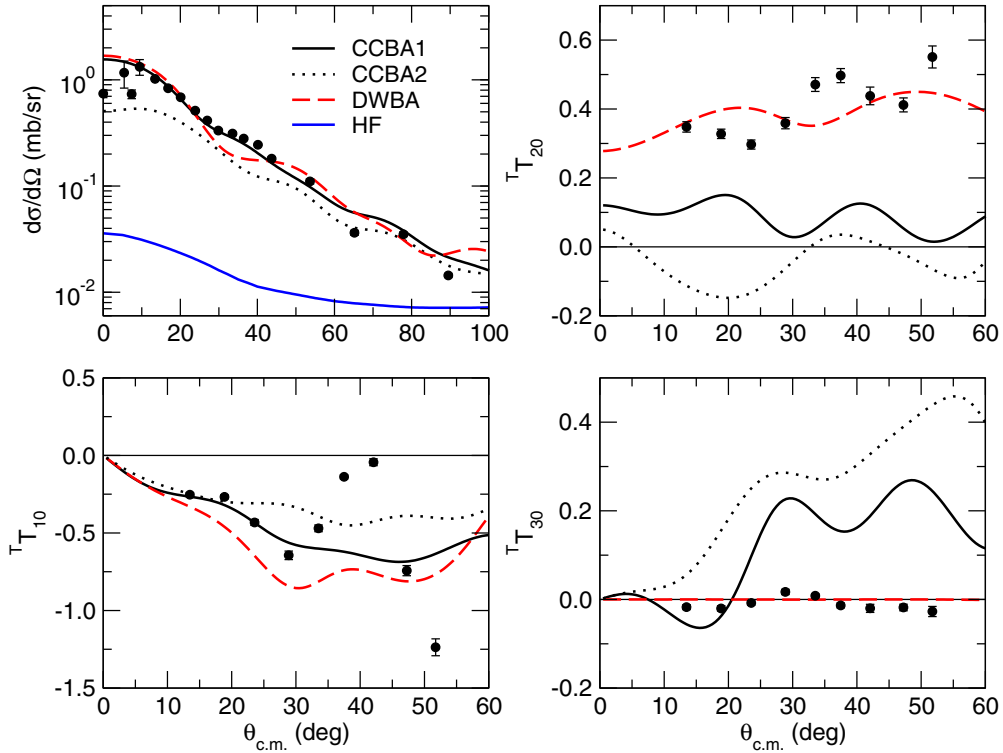
FIG. 5. Cross section and analyzing power angular distributions for the ^{12}C(^{7}Li, t)^{16}O reaction to the 6.92 MeV 2_1^+ state of ^{16}O. The solid black curves denote the CCBA calculation including ground state reorientation and excitation of the 0.478 MeV $1/2^-$ state of ^{7}Li and excitation of the 4.44 MeV 2^+ state of ^{12}C (CCBA1), the dotted black curves the CCBA calculation with additional coupling to the 4.63 MeV $7/2^-$ resonance of ^{7}Li (CCBA2) and the dashed red curve the DWBA calculation. The solid blue curve denotes the Hauser-Feshbach compound nucleus cross section calculated with HELGA which was added incoherently to the CCBA and DWBA cross sections. The calculated analyzing powers are the cross section weighted means of the analyzing powers for the 6.92 MeV 2_1^+ and 7.12 MeV 1_1^- states; see text for details.

a binding energy of 0.001 MeV. This resonance is relatively narrow ($\Gamma = 69$ keV [41]), so this approximation should be reasonably realistic and, in fact, the data of Ref. [35] for population of this resonance are well described by the CC calculation. The results of these calculations are plotted on Figs. 2–8 as the dotted black curves labeled "CCBA2," the cross section angular distributions again being the incoherent sum of the CCBA and HF cross sections and the analyzing powers in Figs. 4 and 5 the cross section weighted means of the analyzing powers for both members of the respective unresolved doublets. The effect of this additional transfer path on the calculated angular distributions is significant, although it worsens the agreement with the cross section data without noticeably improving the description of the analyzing powers (with the exception of $^TT_{10}$ and $^TT_{20}$ for transfer to the 0.0 MeV 0_1^+ state). We note that the effect of this two-step transfer path on the cross section angular distributions is greatest at forward angles ($\theta_{c.m.} < 20°$), the angular region where direct, single-step transfer is usually expected to be dominant.

C. Distorted wave Born approximation calculations

To help assess the importance of two-step contributions, in addition to the CCBA calculations just described we also performed a series of DWBA calculations. The inputs to these

calculations were kept as close as possible to those of the CCBA calculations. All inelastic couplings were omitted and parameter set VII of Table I of Ref. [22] was used as the entrance channel optical model potential. The same spectroscopic amplitudes were used as in the CCBA calculations, although only those concerning the $\langle ^7\text{Li}(3/2^-) \mid \alpha + t \rangle$ and $\langle ^{16}\text{O} \mid \alpha + ^{12}\text{C}(0^+) \rangle$ overlaps were included since DWBA deals only with direct, one-step transitions. All other inputs were identical to those of the corresponding CCBA calculations described in the previous subsection.

The results are plotted in Figs. 2–8 as the dashed red curves. The cross section angular distributions again denote the incoherent sum of the DWBA and HF cross sections and the analyzing powers in Figs. 4 and 5 are the cross section weighted means of the calculated analyzing powers for the 6.05 MeV 0_2^+ and 6.13 MeV 3_1^- states and the 6.92 MeV 2_1^+ and 7.12 MeV 1_1^- states, respectively. The first thing to note is that, with the exception of the 6.05 MeV 0_2^+ (Fig. 3) and 6.92 MeV 2_1^+ (Fig. 5) states, the DWBA cross section angular distributions are significantly different from the CCBA1 results; the CCBA2 cross sections are significantly different from the DWBA results for all states. It is also apparent that the DWBA gives the best overall description of the analyzing powers for all states, although in no case could the description be considered good.
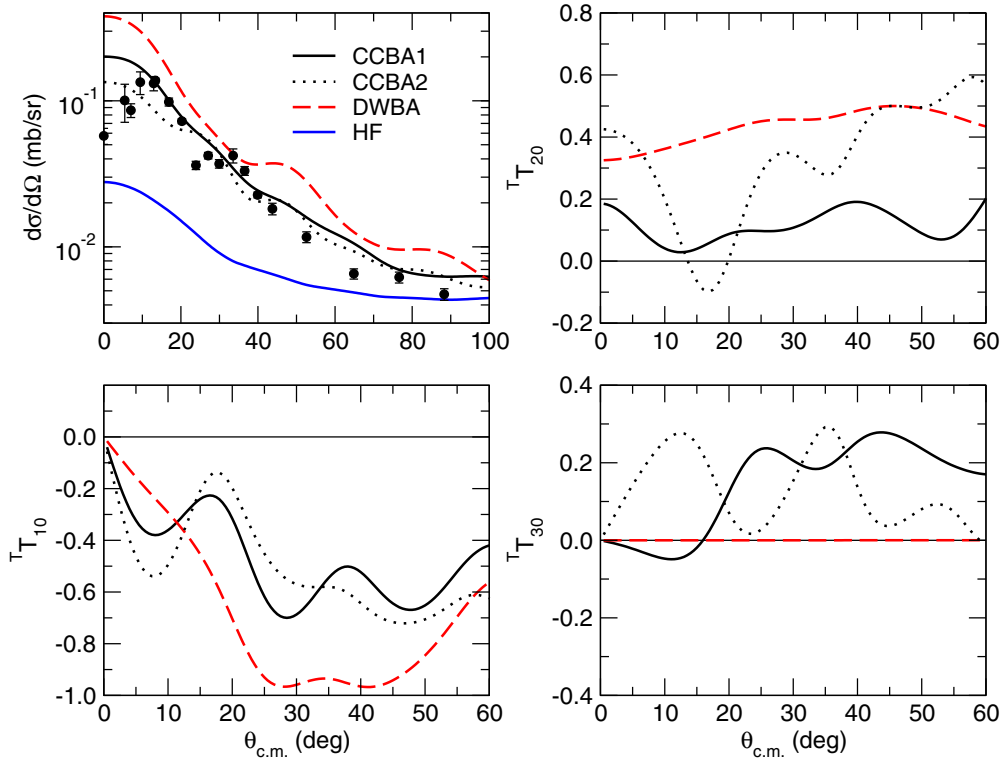
FIG. 6. Cross section and analyzing power angular distributions for the ^{12}C(^{7}Li, t)^{16}O reaction to the 7.12 MeV 1_1^- state of ^{16}O. The solid black curves denote the CCBA calculation including ground state reorientation and excitation of the 0.478 MeV $1/2^-$ state of ^{7}Li and excitation of the 4.44 MeV 2^+ state of ^{12}C (CCBA1), the dotted black curves the CCBA calculation with additional coupling to the 4.63 MeV $7/2^-$ resonance of ^{7}Li (CCBA2) and the dashed red curve the DWBA calculation. The solid blue curve denotes the Hauser-Feshbach compound nucleus cross section calculated with HELGA which was added incoherently to the CCBA and DWBA cross sections.

V. DISCUSSION

As regards the cross section angular distributions, the shell model amplitudes provide a good description of the data when included in the CCBA1 calculations, i.e., when two-step reaction paths proceeding via inelastic excitation of the ^{12}C 4.44 MeV 2^+ and ^{7}Li 0.478 MeV $1/2^-$ states are included. To obtain this agreement only one adjustable parameter per ^{16}O final state is required, viz. the bound-state potential well radius. The analyzing powers are, however, not well described, in particular, the calculated $^T T_{30}$ are much larger than the measured ones over most of the angular range where data exist. A negative relative sign for the spectroscopic amplitude of the $\langle ^7\text{Li}(1/2^-) \mid \alpha + t \rangle$ overlap is essential for the good agreement with the cross section data for transfers to the 0.0 MeV 0_1^+, 6.13 MeV 3_1^-, and 10.35 MeV 4_1^+ states; for transfers to the other levels the impact on the calculated cross section of changing the sign of this amplitude is not significant. Changing the sign of this amplitude affects the calculated analyzing powers significantly for all levels but does not lead to any improvement in their description. The CCBA1 calculations thus appear to confirm empirically the relative sign of the spectroscopic amplitudes for the $\langle ^7\text{Li}(3/2^-) \mid \alpha + t \rangle$ and $\langle ^7\text{Li}(1/2^-) \mid \alpha + t \rangle$ overlaps predicted by Ref. [39]. In Fig. 9 we show the effect of changing the relative sign of these two spectroscopic amplitudes in the CCBA1 calculations as well as removing the transfer path via the ^{7}Li 0.478 MeV $1/2^-$

state altogether on the results for transfer leading to the 0.0 MeV 0_1^+ state of ^{16}O, which shows the greatest sensitivity. Note that ground state reorientation and coupling to the 0.478 MeV $1/2^-$ state of ^{7}Li are still included in the calculation where the transfer via the $1/2^-$ state is switched off. It will be noted that the effect on the cross section is dramatic, completely changing the shape of the angular distribution, although among the analyzing powers only $^T T_{20}$ is affected to a similar extent.

However, the good description of the cross section angular distributions is worsened when the two-step transfer path via the 4.63 MeV $7/2^-$ resonance of ^{7}Li is added. In the calculations labeled as CCBA2 in Figs. 2–8 the relative sign of the spectroscopic amplitude for the $\langle ^7\text{Li}(7/2^-) \mid \alpha + t \rangle$ overlap is again negative, in agreement with the calculations of Ref. [39]; if the sign is changed these calculations completely fail to describe the cross section data. The inclusion of this transfer path can hardly be said to improve the description of the analyzing powers either, with the possible exception of $^T T_{10}$ and $^T T_{20}$ for the 0.0 MeV 0_1^+ state. It is important to note that the addition of this transfer path has most effect on the cross section angular distributions at forward angles ($\theta_{\text{c.m.}} < 20°$), the region which is often assumed to be least sensitive to multistep paths and dominated by one-step, "DWBA"-type transfers. There is clearly destructive interference between the transfer amplitudes here, since the cross sections are
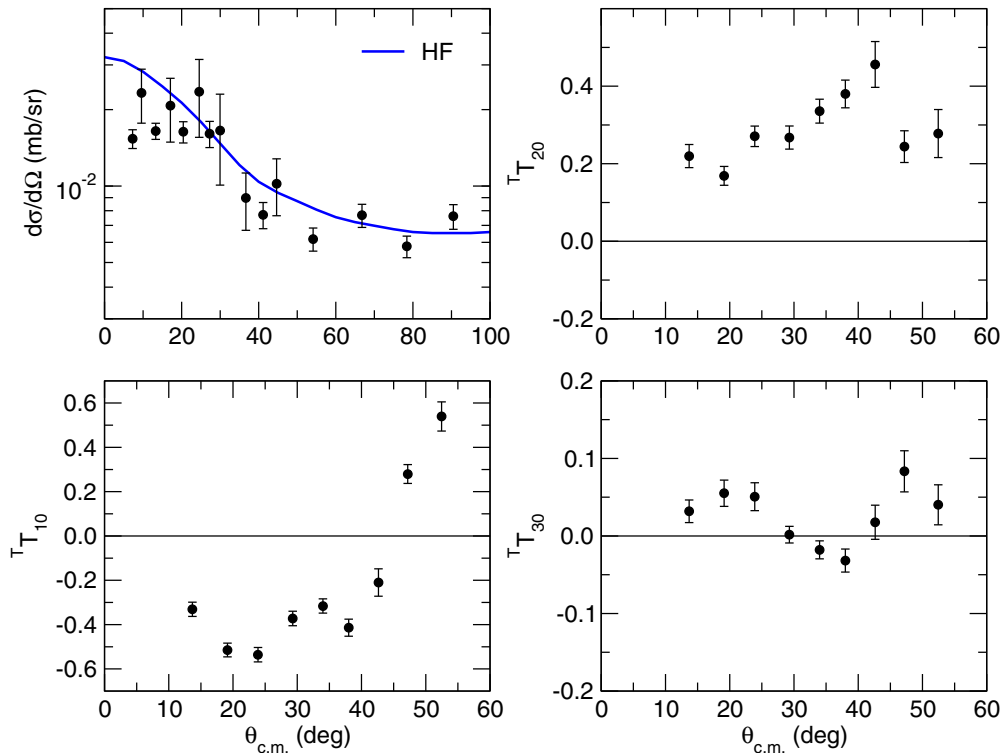
FIG. 7. Cross section and analyzing power angular distributions for the ^{12}C(^{7}Li, t)^{16}O reaction to the 8.87 MeV 2_1^- state of ^{16}O. The solid blue curve denotes the Hauser-Feshbach compound nucleus cross section calculated with HELGA.

significantly reduced in magnitude. This has potentially important consequences for the extraction of "empirical" spectroscopic factors by normalizing DWBA calculations to forward angle cross section angular distributions, as is often done. The present case demonstrates that the assumption underlying this procedure, i.e. that the angular distribution in this region is dominated by the direct one-step transfer, is not always valid.

Presumably, further transfer paths are required to recover the good description of the cross sections; it is already apparent from the poor description of the analyzing powers that neither the CCBA1 nor the CCBA2 calculations include all significant transfer paths. Test calculations in which the spin-orbit term of the empirical $t + {}^{16}$O optical potential of Ref. [42] was added to the exit channel optical potentials (the HT1p global parameters do not include a spin-orbit component) found that it had negligible influence on the cross sections and a small or negligible influence on the analyzing powers, suggesting that the latter could constitute a sensitive probe of the importance of multistep transfer paths. This is supported by the DWBA calculations, also shown in Figs. 2–8, which provide the best overall description of the analyzing powers, particularly $^TT_{30}$. The measured values of this analyzing power are close to zero at all angles for most of the states investigated here, as predicted by the DWBA calculations, and since the CCBA calculations all greatly overpredict its magnitude there must be significant cancellation effects from other transfer paths not included in the present CCBA calculations. Indeed, it can be shown that in the FRDWBA with no spin-dependent distortions, for (^{7}Li, t)

on a 0^+ target leading to a residual nucleus also in a 0^+ state, $^TT_{20} \equiv 1/2$ and $^TT_{30} \equiv 0$ for all angles, see Figs. 2 and 3, so that in these cases at least any deviation from these values must come from spin-dependent components of the potentials (which tests suggest have a small or negligible influence) or multistep transfer paths.

The cross sections predicted by the DWBA calculations also underline the importance of modeling the reaction mechanism as completely as possible. The shapes of the angular distributions calculated with DWBA are in most cases similar to those of the CCBA1 results but the magnitudes are significantly different. The use of DWBA to extract spectroscopic factors in this case could, therefore, lead to erroneous results; of the six levels analyzed in this work the DWBA and CCBA1 calculations give similar results for two only, the 6.05 MeV 0_2^+ and the 6.92 MeV 2_1^+.

Taken overall, our results suggest that further multistep paths in addition to those included in the present calculations play a significant role in the α-particle transfer process in this system. These could include inelastic couplings between the levels of ^{16}O in the exit channel, some of which, e.g., the $0_1^+ \longleftrightarrow 3_1^-$ transition, are known to be strong. However, a test calculation in which this coupling was included in a CCBA calculation including the various α-transfer paths simultaneously to both the 0_1^+ and 3_1^- levels found that it made a negligible difference. It is also in principle possible that transfer paths arising from contributions to the ^{16}O wave functions where the ^{12}C core is in an excited state not included in the present calculations, such as the 9.64 MeV 3_1^-, may make a significant contribution; this state is
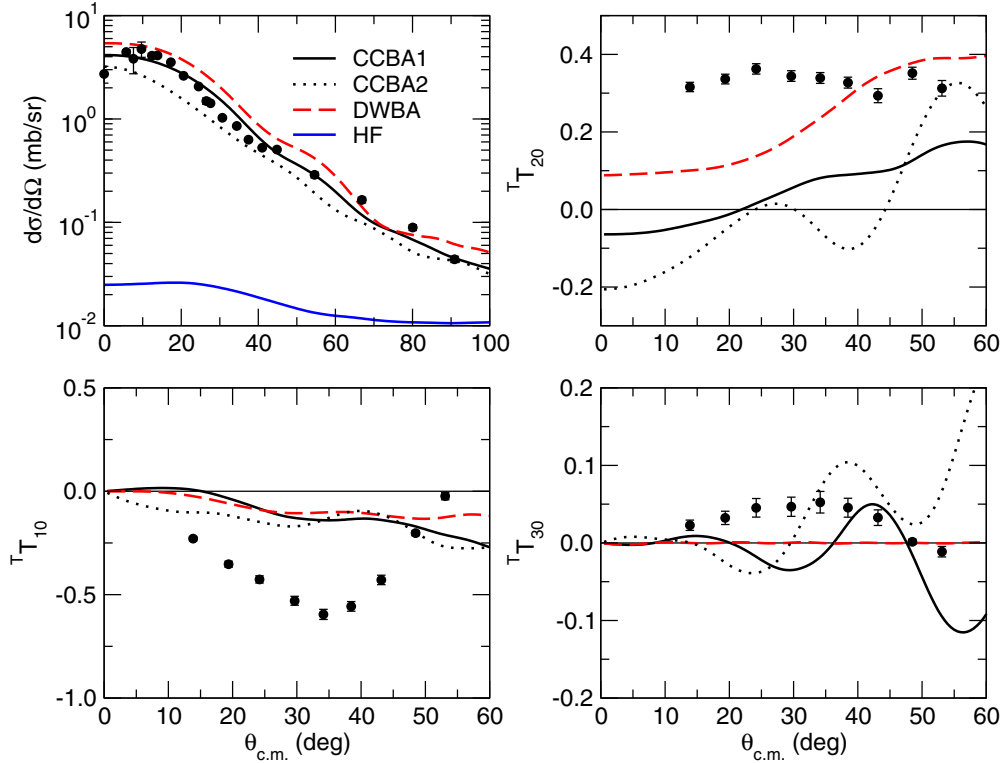
FIG. 8. Cross section and analyzing power angular distributions for the ^{12}C(^{7}Li, t)^{16}O reaction to the 10.35 MeV 4_1^+ state of ^{16}O. The solid black curves denote the CCBA calculation including ground state reorientation and excitation of the 0.478 MeV $1/2^-$ state of ^{7}Li and excitation of the 4.44 MeV 2^+ state of ^{12}C (CCBA1), the dotted black curves the CCBA calculation with additional coupling to the 4.63 MeV $7/2^-$ resonance of ^{7}Li (CCBA2) and the dashed red curve the DWBA calculation. The solid blue curve denotes the Hauser-Feshbach compound nucleus cross section calculated with HELGA which was added incoherently to the CCBA and DWBA cross sections.

certainly populated with a reasonable cross section in the ^{7}Li + ^{12}C interaction at an incident energy of 34 MeV [35]. The final possibility is two-step paths proceeding via further resonant states or the non-resonant continuum of ^{7}Li. The significance of these paths is difficult to assess accurately. The only other resonant state in ^{7}Li of any significance is the 6.68 MeV $5/2^-$, predicted to be weakly populated—it was not observed in Ref. [35]. In addition this state is relatively wide ($\Gamma = 918$ keV [41]) so that it is unclear whether standard methods will be able adequately to handle transfer from this level (this comment also applies to transfers proceeding via non-resonant continuum bins).

Finally, a word concerning the analyzing powers for the 8.87 MeV 2_1^- state. The relatively large measured values might seem incompatible with the good description of the cross section both in terms of shape and magnitude by the HF calculations, since compound nucleus processes are not normally associated with non-zero analyzing powers. However, a small, almost negligible, contribution to the cross section from two-step transfer processes—recall that since this state is of unnatural parity it cannot be populated by direct, one-step α-particle transfer—can nevertheless produce significant analyzing powers; see, e.g., the ^{12}C(^{6}Li, d)^{16}O calculations in Ref. [16]. Similar test calculations of the two-step transfer to this state via the 4.44 MeV 2_1^+ of ^{12}C using the spectroscopic factors of Suzuki [43] confirmed that this is also the case here, yielding cross sections of the order of 10^{-3} mb/sr, i.e.,

an order of magnitude smaller than those observed, while producing analyzing powers of magnitude comparable with the measured ones, although unable to reproduce their shapes.

VI. CONCLUSIONS

The general conclusion of this work must be that, as for the ^{12}C(^{6}Li, d)^{16}O case [16], we are unable to provide a satisfactory description of the analyzing powers for the ^{12}C(^{7}Li, t)^{16}O α-transfer reaction, indicating that there remain additional multistep paths not included in our CCBA calculations which have a significant influence. Nevertheless, a good description of the cross section angular distributions was obtained using a set of spectroscopic amplitudes calculated within a modern shell model framework with one adjustable parameter for each state, viz. the radius of the well binding the transferred α particle to the ^{12}C core, although the inclusion of the transfer path via the 4.63 MeV $7/2^-$ resonance of ^{7}Li worsened this agreement, particularly at forward angles ($\theta_{c.m.} < 20°$). These results lead to the following specific conclusions concerning the current work:

(1) The analyzing powers provide a sensitive probe of the influence of multistep transfer paths on this reaction. This seems particularly the case for the third rank analyzing power $^T T_{30}$, which is experimentally small at all angles measured in this work whereas the calculated values are large, indicating that this observable is
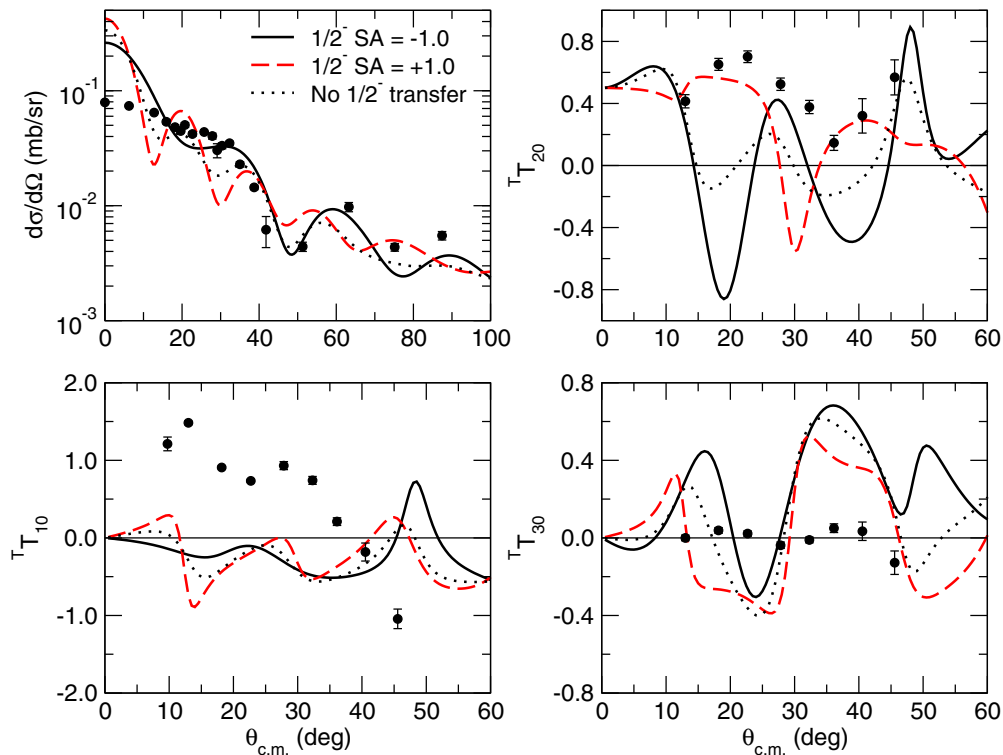
FIG. 9. Cross section and analyzing power angular distributions for the ^{12}C(^{7}Li, t)^{16}O reaction to the 0.0 MeV 0_1^+ state of ^{16}O for CCBA1 calculations with the relative sign of the two $\langle ^7$Li $| \alpha + t \rangle$ overlaps negative (solid black curves), positive (dashed read curves), and with transfer via the ^{7}Li 0.478 MeV $1/2^-$ state omitted (dotted black curves). The cross section angular distributions are the incoherent sums of the CCBA and HF calculations.

presumably the result of a delicate balance of interference effects between different reaction paths and thus sensitive not only to the magnitude but also the phase of their contributions, i.e., to the signs of the relevant spectroscopic amplitudes.

(2) Considering the cross section data alone, our analysis demonstrates the danger of stopping when one has achieved a good description, tempting though this is. Without the analyzing power data the CCBA1 calculations could reasonably have been said to provide about as good a description of the whole data set as is possible, with only the transfers to the 6.05 MeV 2_1^+ and 6.13 MeV 3_1^- states showing room for improvement at angles $\theta_{c.m.} > 40°$. However, the CCBA2 calculations show that adding a single additional transfer path can alter the situation significantly.

(3) Our analysis also demonstrates the need at least to check the influence of multistep transfer paths when attempting to extract spectroscopic information from reaction data of this type. A comparison of the DWBA and CCBA1 curves on Figs. 2–8 shows that, with the exception of the 6.05 MeV 0_2^+ and 6.92 MeV 2_1^+ states, use of DWBA rather than CCBA to extract spectroscopic factors would have lead to significantly smaller values. The CCBA2 results further underline this point since they show that the frequent assumption that the forward angle data at least are dominated by the direct, one-step transfer modeled by the DWBA is not always true.

(4) When including transfer paths that proceed via excited states of the core a set of calculated spectroscopic *amplitudes*, including their signs, is essential since there are too many variables to be determined by adjusting to fit the data. In this respect we are rather attempting to validate the results of a structure model than to extract "empirical" spectroscopic factors, as in a traditional DWBA analysis.

Point 4 contains the essence of our conclusions: If progress is to be made in the analysis of α-transfer reactions of this type, then close collaboration with structure theorists is really required to provide the necessary spectroscopic amplitudes for an analysis of the reaction data that includes as many of the multistep transfer paths as seem necessary; although, see point 2. The procedure adopted in the present analysis, i.e., to take such a set of amplitudes that are then regarded as fixed, use these as input to a reaction calculation and only allow tuning of the radius of the potential well binding the transferred α particle to the core, has much to recommend it, providing as it does a much more direct test of the structure models. For a more rigorous test one would ideally wish to use the actual wave functions provided by the structure models, and this is gradually becoming a practical possibility with modern shell model codes; see, e.g., Refs. [44,45].

Finally, while we have not achieved a completely satisfactory description of the data using the shell model spectroscopic amplitudes, the level of agreement between the

calculations and the data does strongly suggest that these values are realistic. The remaining discrepancies seem more likely to be due to additional multistep transfer paths not included in the present calculations. A similar analysis of the ^{12}C(^{6}Li, d)^{16}O data of Ref. [16] using these amplitudes may prove illuminating in this respect.

[1] S. K. Allison, P. G. Murphy, and E. Norbeck, Phys. Rev. **102**, 1182 (1956).

[2] G. E. Morrison, Phys. Rev. **121**, 182 (1961).

[3] T. A. Tombrello and G. C. Phillips, Phys. Rev. **122**, 224 (1961).

[4] J. E. Wheeler, Phys. Rev. **52**, 1083 (1937).

[5] K. Wildermuth and W. McClure, Springer Tracts Modern Phys. **41** (1966), and references therein.

[6] C. E. Anderson, in *Proceedings of the 2nd Conference on Reactions Between Complex Nuclei, Gatlinburg*, edited by A. Zuker, E. C. Halbert, and F. J. Howard (Wiley, NY, 1960); *ibid*, R. L. Gluckstern and G. Breit.

[7] R. W. Ollerhead, C. Chasman, and D. A. Bromley, Phys. Rev. **134**, B74 (1964).

[8] K. Bethge, K. Meier-Ewert, K. Pfeiffer, and R. Bock, Phys. Lett. B **24**, 663 (1967).

[9] R. Middleton, B. Rosner, D. J. Pullen, and L. Polsky, Phys. Rev. Lett. **20**, 118 (1968).

[10] K. Bethge, Annu. Rev. Nucl. Sci. **20**, 255 (1970).

[11] A. Cunsolo, A. Foti, G. Pappalardo, G. Raciti, and N. Saunier, Phys. Rev. C **18**, 856 (1978).

[12] F. D. Becchetti, J. Jänecke, and C. E. Thorn, Nucl. Phys. A **305**, 313 (1978).

[13] P. T. Debevec, H. T. Fortune, R. E. Segel, and J. F. Tonn, Phys. Rev. C **9**, 2451 (1974).

[14] C. W. Glover and K. W. Kemper, Nucl. Phys. A **366**, 469 (1981).

[15] K. P. Artemov, V. Z. Goldberg, I. P. Petrov, V. P. Rudakov, I. N. Serikov, and V. A. Timofeev, Sov. J. Nucl. Phys. **20**, 368 (1975).

[16] N. Keeley, T. L. Drummer, E. E. Bartosz, C. R. Brune, P. D. Cathers, M. Fauerbach, H. J. Karwowski, K. W. Kemper, B. Kozłowska, E. J. Ludwig, F. Maréchal, A. J. Mendez, E. G. Myers, D. Robson, K. Rusek, and K. D. Veal, Phys. Rev. C **67**, 044604 (2003).

[17] F. Pühlhofer, H. G. Ritter, R. Bock, G. Brommundt, H. Schmidt, and K. Bethge, Nucl. Phys. A **147**, 258 (1970).

[18] M. E. Cobern, D. J. Pisano, and P. D. Parker, Phys. Rev. C **14**, 491 (1976).

[19] F. D. Becchetti, E. R. Flynn, D. L. Hanson, and J. W. Sunier, Nucl. Phys. A **305**, 293 (1978).

[20] C. R. Brune, W. H. Geist, R. W. Kavanagh, and K. D. Veal, Phys. Rev. Lett. **83**, 4025 (1999).

[21] N. Oulebsir, F. Hammache, P. Roussel, M. G. Pellegriti, L. Audouin, D. Beaumel, A. Bouda, P. Descouvemont, S. Fortier, L. Gaudefroy, J. Kiener, A. Lefebvre-Schuhl, and V. Tatischeff, Phys. Rev. C **85**, 035804 (2012).

[22] M. F. Vineyard, J. Cook, K. W. Kemper, and M. N. Stephens, Phys. Rev. C **30**, 916 (1984).

[23] P. D. Cathers, P. V. Green, E. E. Bartosz, K. W. Kemper, F. Maréchal, E. G. Myers, and B. G. Schmidt, Nucl. Instrum. Methods Phys. Res., Sec. A **457**, 509 (2001); **491**, 349(E) (2002).

[24] P. D. Cathers, E. E. Bartosz, M. W. Cooper, N. Curtis, K. W. Kemper, F. Maréchal, E. G. Myers, B. G. Schmidt, K. Rusek, and V. Hnizdo, Phys. Rev. C **63**, 064601 (2001).

[25] E. E. Bartosz, N. Keeley, P. D. Cathers, M. W. Cooper, K. W. Kemper, F. Maréchal, and K. Rusek, Phys. Rev. C **64**, 014606 (2001).

[26] A. Volya and Yu. M. Tchuvil'sky, Phys. Rev. C **91**, 044319 (2015).

[27] Y. Utsuno and S. Chiba, Phys. Rev. C **83**, 021301(R) (2011).

[28] K. Kravvaris and A. Volya, Phys. Rev. Lett. **119**, 062501 (2017).

[29] K. Kravvaris, Ph.D. thesis, Florida State University, 2018.

[30] H. V. Klapdor, H. Reiss, and G. Rosner, Nucl. Phys. A **262**, 157 (1976).

[31] L. C. Dennis, A. Roy, A. D. Frawley, and K. W. Kemper, Nucl. Phys. A **359**, 455 (1981).

[32] S. K. Penny, Oak Ridge National Laboratory (unpublished).

[33] I. J. Thompson, Comput. Phys. Rep. **7**, 167 (1988).

[34] S. Raman, C. W. Nestor, and P. Tikkanen, At. Data Nucl. Data Tables **78**, 1 (2001).

[35] J. Cook, M. N. Stephens, K. W. Kemper, and A. K. Abdallah, Phys. Rev. C **33**, 915 (1986).

[36] A. Weller, P. Egelhof, R. Čaplar, O. Karban, D. Krämer, K. H. Möbius, Z. Moroz, K. Rusek, E. Steffens, G. Tungate, K. Blatt, I. Koenig, and D. Fick, Phys. Rev. Lett. **55**, 480 (1985).

[37] D. Y. Pang, W. M. Dean, and A. M. Mukhamedzhanov, Phys. Rev. C **91**, 024611 (2015).

[38] B. Buck and A. C. Merchant, J. Phys. G **14**, L211 (1988).

[39] O. F. Nemets *et al.*, *Nucleon Clusters in Atomic Nuclei and Many-Nucleon Transfer Reactions* (in Russian) (Ukrainian Academy of Sciences, Institute for Nuclear Research, Kiev, 1988).

[40] T. Fukui, Y. Kanada-En'yo, K. Ogata, T. Suhara, and Y. Taniguchi, Nucl. Phys. A **983**, 38 (2019).

[41] D. R. Tilley, C. M. Cheves, J. L. Godwin, G. M. Haled, H. M. Hofmann, J. H. Kelley, C. G. Sheu, and H. R. Weller, Nucl. Phys. A **708**, 3 (2002).

[42] J. B. A. England, L. Zybert, G. T. A. Squier, O. Karban, R. Zybert, J. M. Nelson, D. Barker, B. R. Fulton, M. C. Mannion, C. A. Ogilvie, L. Potvin, C. Pinder, C. O. Blyth, G. C. Morrison, G. J. Pyle, S. Roman, N. M. Clarke, K. I. Pearce, P. J. Simmonds, R. J. Griffiths, D. L. Watson, M. D. Cohler, R. Wadsworth, J. O'Donnell, and M. Smithson, Nucl. Phys. A **475**, 422 (1987).

[43] Y. Suzuki, Prog. Theor. Phys. **55**, 1751 (1976).

[44] F. Flavigny, A. Gillibert, L. Nalpas, A. Obertelli, N. Keeley, C. Barbieri, D. Beaumel, S. Boissinot, G. Burgunder, A. Cipollone, A. Corsi, J. Gibelin, S. Giron, J. Guillot, F. Hammache, V. Lapoux, A. Matta, E. C. Pollacco, R. Raabe, M. Rejmund, N. de Séreville, A. Shrivastava, A. Signoracci, and Y. Utsuno, Phys. Rev. Lett. **110**, 122503 (2013).

[45] F. Flavigny, N. Keeley, A. Gillibert, and A. Obertelli, Phys. Rev. C **97**, 034601 (2018).